Applied Physics Letters

Graphene/gallium arsenide-based Schottky junction solar cells

Cite as: Appl. Phys. Lett. **103**, 233111 (2013); https://doi.org/10.1063/1.4839515
Submitted: 14 October 2013 . Accepted: 19 November 2013 . Published Online: 05 December 2013

Wenjing Jie, Fengang Zheng, and Jianhua Hao

Graphene/gallium arsenide-based Schottky junction solar cells

Wenjing Jie, Fengang Zheng, and Jianhua Hao[a)]
Department of Applied Physics, The Hong Kong Polytechnic University, Hung Hom, Hong Kong, People's Republic of China

(Received 14 October 2013; accepted 19 November 2013; published online 5 December 2013)

Chemical-vapor-deposited single- and bi-layer graphene sheets have been transferred onto n-type GaAs substrates. The rectifying characteristics and photovoltaic behaviors of graphene/GaAs junctions have been systematically investigated. The graphene sheets can be combined with the underlying n-type GaAs substrates to form Schottky junctions. For bilayer graphene, the Schottky junction shows photovoltaic effects with the open-circuit voltage of 0.65 V and the short-circuit current density of 10.03 mA/cm^2, yielding a power conversion efficiency of 1.95%, which are superior to single-layer one. Such performance parameters are comparable to those of other pristine graphene/semiconductor junction-based devices. © *2013 AIP Publishing LLC*. [http://dx.doi.org/10.1063/1.4839515]

Due to its unique properties of high optical transmittance, mechanical flexible and fascinating electric characteristics, such as low resistivity, ultra-high mobility, near-zero band gap, graphene has been regarded as one of the promising materials for photovoltaic devices applications.[1–5] In principle, any semiconductor with a moderate carrier density can form a Schottky junction with a certain metal if the difference between their work functions is large enough.[6] Graphene, as a semi-metal, can serve as active layer (metal) to form metal/semiconductor (M/S) Schottky diode with some semiconductors, such as Si, SiC, GaAs, GaN, and graphene oxide.[7–12] Based on the M/S diode, Li *et al*. reported graphene/Si Schottky junction solar cells with the average power conversion efficiency (PCE) of about 1.65% and open-circuit voltage of $0.42 \sim 0.48$ V by transferring graphene sheets onto n-type Si.[13,14] Followed by this work, the graphene/Si heterojunction solar cells have been extensively studied.[15–18] Accordingly, many efforts have been paid to improve the performance of graphene-based Schottky junction solar cells by using an antireflection technique, modifying the work function of graphene,[19] chemical or substitutional doping to graphene layer,[20,21] or using the colloidal antireflection TiO_2 coating layer onto graphene/Si.[22] As a result, the PCE value has been greatly improved even up to 14.5%. Additionally, the Schottky junction solar cells can be fabricated by combining graphene with other semiconductor nanostructures like CdS nanowire and CdSe nanobelt exhibiting the PCE of approximately 1.5%.[23,24]

In comparison with currently widely used Si, GaAs has the merits of higher saturated electron mobility and direct band gap.[25–27] Besides, GaAs is highly resistant to radiation damage, which makes GaAs solar cells take over from silicon as the conventional cell type desirable for space applications. The present technique can also provide the possibility to combine large-area graphene with GaAs.[8,28,29] Moreover, theoretical simulation shows that graphene/GaAs heterojunction has a potential of exhibiting superior photovoltaic behaviors to those of graphene/Si junctions.[30] Unfortunately, graphene/GaAs Schottky junction solar cells have not been presented until now. In this work, chemical-vapor-deposited single-layer graphene (SLG) and bilayer graphene (BLG) flakes have been transferred onto n-type GaAs substrates. The contact behaviors, rectifying characteristics and photovoltaic effects of graphene/GaAs heterojunctions have been systematically investigated.

The junction device is schematically shown in Fig. 1(a). Before transferring graphene, low-resistance Au contacts were grown on the back side of the GaAs substrates by thermal evaporation. Then, a 200 nm-thick SiO_2 layer was deposited on the substrate by magnetron sputtering at 120 °C using a defined mask to form a GaAs channel with a width of 1 mm which will be used to contact with graphene. After the growth of SiO_2 layer, wafer-scale SLG and BLG sheets prepared by chemical vapor deposition (CVD) method were transferred onto the n-GaAs substrates with the resistivity of $1.2 \sim 1.6 \times 10^3$ Ω cm. The detailed transfer process can refer to our earlier studies.[31,32] Owing to its good mechanical properties, the graphene sheet could be continuous across the patterned steps between the SiO_2 layers and GaAs channel to form a junction with the area of about 1 mm × 1 mm. And more importantly, the graphene flakes could tightly adhere to the underlying GaAs substrates and maintain in good contact without air bubbles at the interface of the junction. Then, the silver paste was employed to serve as top electrodes on

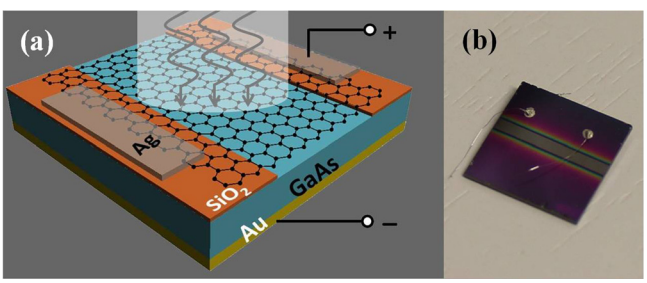

FIG. 1. (a) The schematic of Ag/graphene/GaAs/Au hybrid system with SiO_2 as an insulating layer. (b) Photograph of the graphene/GaAs junction solar cell.

a)Author to whom correspondence should be addressed. Electronic mail: jh.hao@polyu.edu.hk

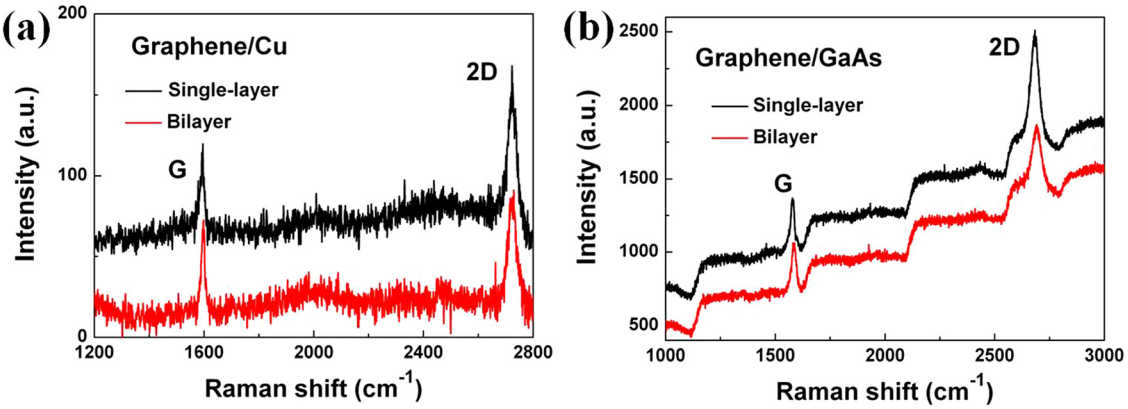

FIG. 2. Raman spectra of both single- and bilayer graphene sheets on (a) copper foils, (b) GaAs substrates.

graphene. The SiO_2 layer functioned as an insulating layer to prevent the formation of contact between the top electrode of Ag and the semiconductor GaAs considering the discontinuity of large-area graphene prepared by CVD. Fig. 2(b) shows the photograph of two pieces of graphene sheets transferred onto the GaAs substrate (10 mm × 10 mm × 0.5 mm) to form two individual solar cell devices. The graphene flakes on Cu and GaAs substrates were characterized by Raman spectroscopy (HORIBA, HR800) with the excitation wavelength of 488 nm. The current–voltage (I–V) data were recorded using a Keithley 2400 SourceMeter. The forward bias was defined as positive voltage applied to the graphene. The photovoltaic effects of the devices were tested with a solar simulator (Thermo Oriel 91192-1000) under conditions of air mass 1.5 (AM 1.5) illumination. All the above measurements were performed in air ambient at room temperature.

Figs. 2(a) and 2(b) compare of Raman spectra between the SLG and BLG before and after transferred onto the GaAs substrates. The most intense features of G and 2D peaks can be clearly observed in all Raman spectra. For the graphene on GaAs, sharp 2D peak lies at about 2682 cm^{-1} (2689 cm^{-1}) with full-width-at-half maximum (FWHM) of about 46 cm^{-1} (54 cm^{-1}) for single-layer (bilayer) graphene. No defect-related D peak is detected, confirming the absence of significant defects in the graphene sheets.[33] For SLG, the 2D peak is approximately 2 times the height of G peak. Meanwhile, BLG exhibits relatively low 2D intensity with the slight red shift of the 2D position in comparison with SLG. Thus, we can conclude that SLG and BLG sheets are transferred onto GaAs substrates, respectively.

Fig. 3(a) shows the dark and light J–V curves of SLG/GaAs junction solar cell with a rectification ratio of about 24 when the voltage $V = \pm 1$ V, suggesting a Schottky junction is formed between the SLG and n-GaAs. The doping concentration of n-GaAs is about 5×10^{17} cm^{-3} and the work function of n-type GaAs ($\Phi_{n\text{-}GaAs}$) is about 4.11 eV. The J–V curve of SLG-based solar cell exhibits a down-shift curve with the short-circuit current density (J_{sc}) and open-circuit voltage (V_{oc}) of 6.43 mA/cm^2 and 0.62 V, respectively, yielding the PCE of 1.09% with the fill factor

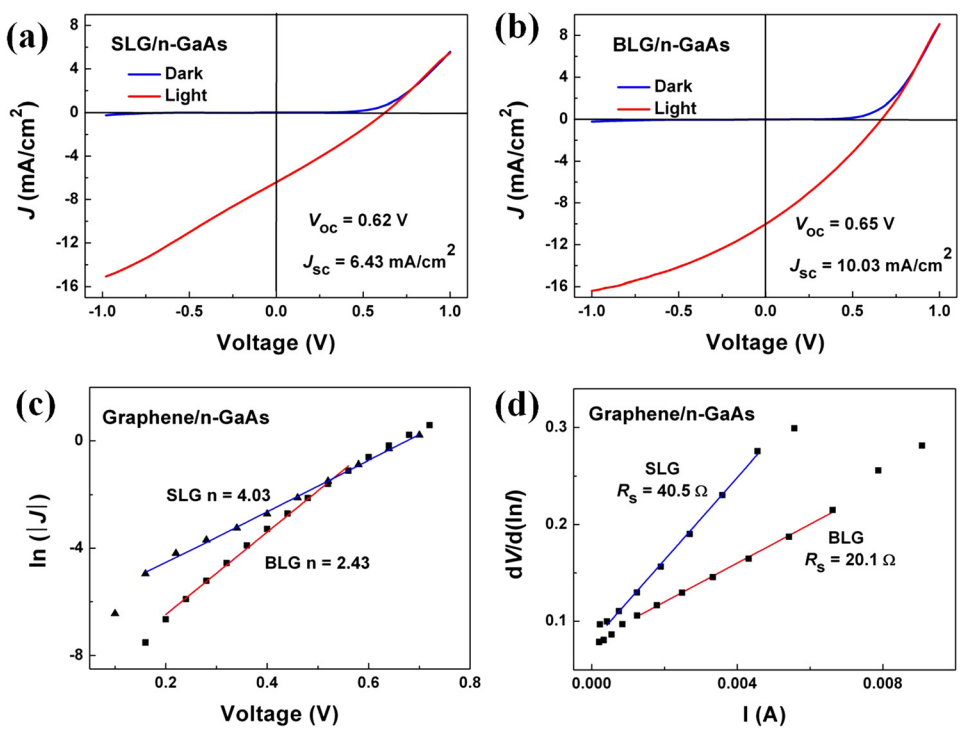

FIG. 3. The dark and light current density–voltage curves of the heterojunctions of (a) SLG/n-GaAs, (b) BLG/n-GaAs. The linear fit (c) to the ln(|J|)–V curve, (d) to the line of dV/dln$I$ vs. I for both SLG/n-GaAs and BLG/n-GaAs Schottky junctions.

(*FF*) of about 0.27. On the other hand, for BLG, the dark *J*–*V* curve exhibits enhanced rectifying characteristics with a rectification ratio of about 43 when $V = \pm 1$ V. Accordingly, the BLG-based Schottky junction shows superior photovoltaic effects to SLG. Not only the J_{sc} and V_{oc} are improved to 10.03 mA/cm^2 and 0.65 V, respectively, but also higher PCE of 1.95% and *FF* of 0.30 are obtained, as shown in Fig. 3(b). Although the present value of *FF* seems not large, further improvement is required via some potential methods, such as optimizing process and reducing graphene/GaAs interface states responsible for high surface recombination possibilities as well as chemical doping. At any rate, BLG/n-GaAs solar cell here shows a comparable performance (J_{sc}, V_{oc} PCE) in comparison to other pristine graphene/semiconductor (such as Si, CdS, and CdSe.) junction-based devices reported so far. In particular, both SLG and BLG based graphene/n-GaAs heterojunction solar cells are capable of exhibiting a relatively large V_{oc} compared to their other semiconductor counterparts where V_{oc} is usually not higher than 0.6 V.[13,23,24] Besides, the PCE value of the device is maintained over a period of more than four months in air ambient, implying excellent stability of the device.

To fully understand the Schottky junction behaviors, the *J*–*V* curves of SLG/GaAs and BLG/GaAs device in dark have been studied. The rectifying behavior of M/S junction over the Schottky barrier at the interface is well described by classic thermionic-emission theory and can be expressed as

$$J(V) = J_s\left[\exp\left(\frac{eV}{nk_BT}\right) - 1\right], \tag{1}$$

where J_s is the reverse saturation current density, e is electronic charge, n is the diode ideality factor, k_B is the Boltzman constant, T is the absolute temperature. The nearly linear fit to the $\ln(|J|)$–V curves with the voltage in the range of 0.2 to 0.7 V of SLG- and BLG-based Schottky junctions can be obtained, as shown in Fig. 3(c). According to the slope of the fitting line, we can deduce the diode ideality factor of 4.03 and 2.43 for SLG- and BLG-based Schottky junction, respectively. Additionally, J_s can be described as

$$J_s = A^*T^2\exp\left(-\frac{e\Phi_b}{k_BT}\right), \tag{2}$$

where A* is the effective Richardson's constant of GaAs.[34] Then the Schottky-barrier height is calculated to be about 0.68 and 0.75 eV for SLG- and BLG-based junctions, respectively. Furthermore, series resistance R_s of the diode can be extracted by plotting the line of $dV/d\ln I$ as a function of I [Fig. 3(d)]. The slope of the linear fitting to the curves gives rise to R_s of 40.5 Ω for SLG diode which is twice larger than that (20.1 Ω) of BLG with the contact area of about 0.01 cm^2 according to Eq. (3)

$$I = I_s\exp\left(\frac{e(V - IR_s)}{nk_BT}\right). \tag{3}$$

To analyze the underlying mechanism of the graphene/GaAs junction qualitatively, the energy band diagram of the junction is plotted (Fig. 4). Theoretically, n-GaAs with electron affinity ($\chi = 4.07$ eV) lower than the work function of graphene (Φ_G) creates an M/S diode with

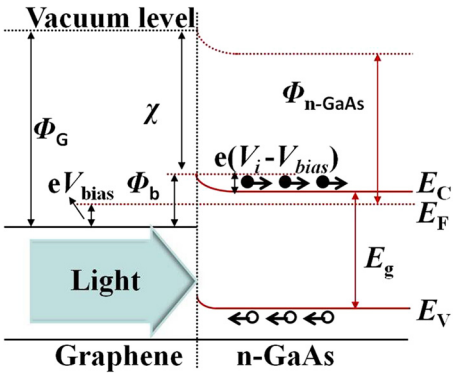

FIG. 4. The energy band diagram of graphene/n-GaAs Schottky junction solar cell at the interface under illumination. E_C, E_V, E_F correspond to the conduction band edge, valence band edge, and Fermi level of n-GaAs, respectively. E_g stands for the energy gap.

Schottky-barrier height ($\Phi_b = \Phi_G - \chi$), giving rise to the rectification behaviors of the graphene/n-GaAs junction. Subsequently, a build-in potential ($eV_i = \Phi_G - \Phi_{n\text{-}GaAs}$) is generated in n-GaAs adjacent to the interface due to the different work function of graphene and n-GaAs. A space-charge region is formed accompanied by the build-in voltage (V_i) in the semiconductor near the interface. Under illumination, the carriers (electron and hole) excited by photons are separated and subsequently transported to the electrodes, yielding photovoltaic effects from such junction devices. In principle, the graphene layer not only serves as transparent electrodes for the junction solar cell but also contributes to carrier separation and transport.

In our experiments, BLG-based device shows better photovoltaic performance compared to SLG-based one exhibiting unexpectedly large ideality factor, high series resistance and low Schottky-barrier height. Our results is consistent with previously reported graphene-Si solar cells, in which multilayer graphene device can exhibit better conversion efficiency compared to its single-layer counterpart.[35] From theoretical consideration, the large series resistance of SLG/GaAs heterojunction can be a major factor for suppressing the carrier separation and transport. Moreover, the high Schottky barrier should be benefit to enhance the performance of BLG/GaAs solar cell. Specifically, when the Schottky barrier is larger, the recombination of the photo-generated electron and hole is more difficult to occur at the interface of the graphene/GaAs. Besides, SLG is believed to have little contribution to the formation of the depletion layer in the Schottky junction by considering the one-atom thickness of the graphene layer.[35] As a consequence, the photo-generated charges could be readily recombined each other, leading to lower *FF* value and the degraded performance of SLG/GaAs in our experiments. Another potential reason is that there are inevitably some holes existing in the SLG during the growth and transfer process, giving rise to the reduction of the contact area and increasing the possibility to the diffusion of air and water into the device from the atmosphere.[36] However, the possibility of the hole existence is dramatically reduced in BLG, resulting in the enhancement of photovoltaic performance.

In summary, n-type GaAs has been combined with graphene layers to form Schottky junctions. We have

demonstrated photovoltaic characteristics of graphene-on-GaAs Schottky junction with the V_{oc} of 0.65 V, J_{sc} of 10.03 mA/cm^2 and PCE value of 1.95%. Our characterization and calculations of the rectifying characteristics of the diodes suggest that bilayer graphene/GaAs junction exhibits smaller ideality factor (2.43), higher Schottky barrier height (0.75 eV), and lower series resistance (20.1 Ω) compared to single-layer one, which can give rise to the improved photovoltaic behaviors of BLG-based junction solar cells. This work implies that the fabricated graphene/GaAs system is promising for photovoltaic applications by considering the high-performance of optoelectronic capabilities of radiation-resistant GaAs wafer.

This research was supported in part by a grant from the Research Grants Council of Hong Kong (GRF Project No. PolyU500910) and PolyU Postgraduate Scholarship (RT6F).

[1]Y. Wang, S. W. Tong, X. F. Xu, B. Özyilmaz, and K. P. Loh, Adv. Mater. **23**, 1514 (2011).
[2]L. Gomez De Arco, Y. Zhang, C. W. Schlenker, K. Ryu, M. E. Thompson, and C. Zhou, ACS Nano **4**, 2865 (2010).
[3]Z. Liu, J. Li, Z.-H. Sun, G. Tai, S.-P. Lau, and F. Yan, ACS Nano **6**, 810 (2012).
[4]C. X. Guo, G. H. Guai, and C. M. Li, Adv. Energy Mater. **1**, 448 (2011).
[5]X. Huang, Z. Zeng, Z. Fan, J. Liu, and H. Zhang, Adv. Mater. **24**, 5979 (2012).
[6]Y. Ye and L. Dai, J. Mater. Chem. **22**, 24224 (2012).
[7]S. Tongay, T. Schumann, X. Miao, B. R. Appleton, and A. F. Hebard, Carbon **49**, 2033 (2011).
[8]S. Tongay, T. Schumann, and A. F. Hebard, Appl. Phys. Lett. **95**, 222103 (2009).
[9]S. Tongay, M. Lemaitre, T. Schumann, K. Berke, B. R. Appleton, B. Gila, and A. F. Hebard, Appl. Phys. Lett. **99**, 102102 (2011).
[10]C.-C. Chen, C.-C. Chang, Z. Li, A. F. J. Levi, and S. B. Cronin, Appl. Phys. Lett. **101**, 223113 (2012).
[11]X. Wu, M. Sprinkle, X. Li, F. Ming, C. Berger, and W. de Heer, Phys. Rev. Lett. **101**, 026801 (2008).
[12]C.-C. Chen, M. Aykol, C.-C. Chang, A. F. J. Levi, and S. B. Cronin, Nano Lett. **11**, 1863 (2011).
[13]X. Li, H. Zhu, K. Wang, A. Cao, J. Wei, C. Li, Y. Jia, Z. Li, X. Li, and D. Wu, Adv. Mater. **22**, 2743 (2010).
[14]R. Won, Nature Photon. **4**, 411 (2010).
[15]Y. Shi, K. K. Kim, A. Reina, M. Hofmann, L.-J. Li, and J. Kong, ACS Nano **4**, 2689 (2010).
[16]T. Feng, D. Xie, Y. Lin, Y. Zang, T. Ren, R. Song, H. Zhao, H. Tian, X. Li, H. Zhu, and L. Liu, Appl. Phys. Lett. **99**, 233505 (2011).
[17]Z. Li, H. Zhu, D. Xie, K. Wang, A. Cao, J. Wei, X. Li, L. Fan, and D. Wu, Chem. Commun. **47**, 3520 (2011).
[18]X. Li, D. Xie, H. Park, M. Zhu, T. H. Zeng, K. Wang, J. Wei, D. Wu, J. Kong, and H. Zhu, Nanoscale **5**, 1945 (2013).
[19]Y. Lin, X. Li, D. Xie, T. Feng, Y. Chen, R. Song, H. Tian, T. Ren, M. Zhong, K. Wang, and H. Zhu, Energy Environ. Sci. **6**, 108 (2013).
[20]X. Miao, S. Tongay, M. K. Petterson, K. Berke, A. G. Rinzler, B. R. Appleton, and A. F. Hebard, Nano Lett. **12**, 2745 (2012).
[21]X. Li, L. Fan, Z. Li, K. Wang, M. Zhong, J. Wei, D. Wu, and H. Zhu, Adv. Energy Mater. **2**, 425 (2012).
[22]E. Shi, H. Li, L. Yang, L. Zhang, Z. Li, P. Li, Y. Shang, S. Wu, X. Li, J. Wei, K. Wang, H. Zhu, D. Wu, Y. Fang, and A. Cao, Nano Lett. **13**, 1776 (2013).
[23]Y. Ye, L. Gan, L. Dai, Y. Dai, X. Guo, H. Meng, B. Yu, Z. Shi, K. Shang, and G. Qin, Nanoscale **3**, 1477 (2011).
[24]Y. Ye, Y. Dai, L. Dai, Z. Shi, N. Liu, F. Wang, L. Fu, R. Peng, X. Wen, Z. Chen, Z. Liu, and G. Qin, ACS Appl. Mater. Interfaces **2**, 3406 (2010).
[25]W. Huang, Z. P. Wu, and J. H. Hao, Appl. Phys. Lett. **94**, 032905 (2009).
[26]X. H. Wei, W. Huang, Z. B. Yang, and J. H. Hao, Scr. Mater. **65**, 323 (2011).
[27]Z. Y. Yang and J. H. Hao, J. Appl. Phys. **112**, 054110 (2012).
[28]S. Tongay, M. Lemaitre, X. Miao, B. Gila, B. Appleton, and A. F. Hebard, Phys. Rev. X **2**, 011002 (2012).
[29]A. M. Munshi, D. L. Dheeraj, V. T. Fauske, D.-C. Kim, A. T. J. van Helvoort, B.-O. Fimland, and H. Weman, Nano Lett. **12**, 4570 (2012).
[30]S. K. Behura, P. Mahala, A. Ray, I. Mukhopadhyay, and O. Jani, Appl. Phys. A **111**, 1159 (2013).
[31]W. J. Jie, Y. Y. Hui, Y. Zhang, S. P. Lau, and J. H. Hao, Appl. Phys. Lett. **102**, 223112 (2013).
[32]W. J. Jie, Y. Y. Hui, N. Y. Chan, Y. Zhang, S. P. Lau, and J. H. Hao, J. Phys. Chem. C **117**, 13747 (2013).
[33]A. C. Ferrari, J. C. Meyer, V. Scardaci, C. Casiraghi, M. Lazzeri, F. Mauri, S. Piscanec, D. Jiang, K. S. Novoselov, S. Roth, and A. K. Geim, Phys. Rev. Lett. **97**, 187401 (2006).
[34]M. Missous, E. H. Rhoderick, D. A. Woolf, and S. P. Wilkes, Semicond. Sci. Technol. **7**, 218 (1992).
[35]X. Li, D. Xie, H. Park, T. H. Zeng, K. Wang, J. Wei, M. Zhong, D. Wu, J. Kong, and H. Zhu, Adv. Energy Mater. **3**, 1029 (2013).
[36]Z. Liu, J. Li, and F. Yan, Adv. Mater. **25**, 4296 (2013).